

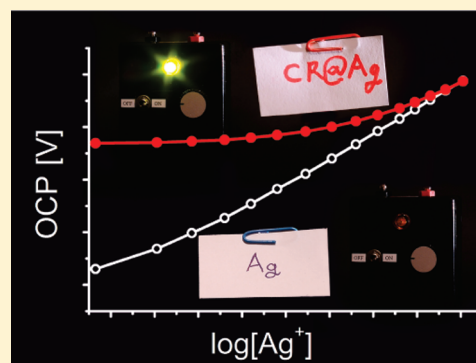
# Organics@metals as the Basis for a Silver/Doped-Silver Electrochemical Cell

Ofer Sinai and David Avnir\*

Institute of Chemistry, The Hebrew University of Jerusalem, Jerusalem 91904, Israel

**ABSTRACT:** Classically, an electrochemical cell is constructed from a pair of different metals. Here we demonstrate a new concept: An electrochemical cell in which the two electrodes are made of the same metal. This has been made possible by employing the new methodology of organic doping of metals in the preparation of one of the electrodes. Specifically, pure silver and silver doped with Congo-red (CR) were used. The alteration of the electrode behavior of silver by incorporation of the organic dopant was revealed by potentiometry and cyclic voltammetry: Potentiometry showed that the entrapment of CR inhibits the response of silver to silver ions; voltammetry indicated a 30-fold increase of the reduction current measured at the electrode surface during cathodic sweeps. On the basis of this, we constructed an electrochemical cell in which the potential difference between pure and doped silver electrodes was used to activate a light-emitting diode in an external circuit.

**KEYWORDS:** organics@metals, potentiometry, cyclic voltammetry



## BACKGROUND

Work in recent years—first described in this journal<sup>1</sup>—involving the irreversible entrapment of organic molecules, polymers, catalysts, and enzymes in metal matrixes has led to the establishment of a new family of composite materials, the organics@metals family.<sup>2–7</sup> To allow the intact entrapment of the organic element, termed a “dopant”, a room-temperature, one-pot methodology has been developed. This involves the reduction of metal ions from solution, which leads to the formation of metal nanocrystallites and subsequently to their aggregation into mesoporous, metallic matrixes. The products preserve some of their metal properties such as metallic sheen and crystalline tight-packed structure. The porosity is primarily interstitial, that is, pores are formed in between tightly aggregated, pure-metal crystals. As a result of being present in the solution of metal ions before and during reduction and aggregation, the dopant is incorporated intact into inter-crystallite cages. Furthermore, its removal by subsequent washing with the solvent used for the synthesis is rendered practically impossible, despite the fact that the dopant is originally soluble in this solvent. This is termed “entrapment”. However, dopants have been found to remain accessible, via diffusion through the metal matrix pore system, to extraction with more effective solvents<sup>1,6,8</sup> and to reactions with external reagents.<sup>1,3,4,9,10</sup> So far, entrapment of a variety of organic molecules has been successfully achieved in several different metals, from aqueous and organic media, and with reduction carried out by homogeneous reductants (e.g., sodium hypophosphite<sup>1</sup> or *N,N*-dimethylformamide<sup>11</sup>), by dispersed metal powders according to the electrochemical series,<sup>8</sup> or electrolytically.<sup>6</sup> The diversity of these conditions demonstrates the ubiquity of the entrapment phenomenon. The amount of organic content varies according to synthesis conditions, but is generally estimated to be about 1%

weight, or a few hundred metal atoms per one organic unit, and at most about 10% in weight.<sup>11</sup>

Entrapment allows the fine-tuning of metal properties and their tailoring with induced properties from the huge selection of organic and biological molecules at the disposal of science today. Several studies have demonstrated the alteration of the metal matrix’ physical properties: the metal composite’s electrical conductivity has been shown to be a function of its loading and the nature of the dopant,<sup>5,11</sup> and the entrapment of chiral dopants has led to the induction of chirality in bulk metal (which is of course normally achiral).<sup>4,12</sup> In addition, it has been found that the inherent catalytic behavior of a metal may be modified by doping.<sup>4,13</sup>

In this research, it is demonstrated that the electrode behavior of a metal, and in particular its apparent electrode potential, may also be altered by doping it with an organic element. This is done mainly through the examination of potentiometric and voltammetric behavior of silver, pure or doped with Congo red (CR). The interest is 2-fold: both the feasibility of altering another basic property of the metal, and the potential to mitigate metal corrosion, in view of the enormous economic impact that corrosion has on society (e.g., as of 2001, the direct costs alone of corrosion in the U.S. have been estimated at \$276 billion per annum, more than 3.1% of the gross domestic product<sup>14</sup>).

## EXPERIMENTAL SECTION

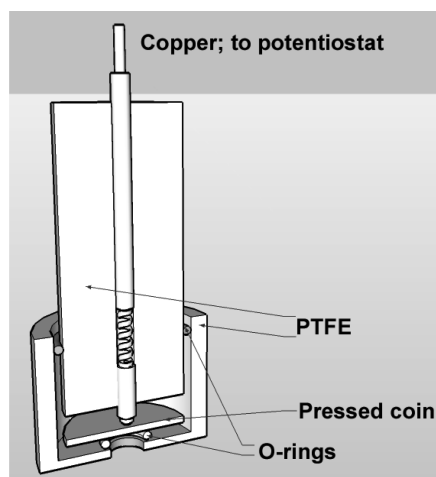
**Chemicals.** Congo red (certified, dye content 97%) was from Aldrich. Silver nitrate (ACS reagent) was from Acros Organics.

**Received:** January 9, 2011

**Revised:** May 29, 2011

**Published:** June 30, 2011

Scheme 1. Working Electrode Setup



Potassium nitrate (ACS reagent) was from Reidel-de Haen, sodium hypophosphite hydrate from Aldrich. All electrochemical analyses were performed in triple distilled water (TDW, conductivity typically no more than  $0.056 \mu\text{S}/\text{cm}$ ).

**Entrapment of CR in Silver.** On the basis of the procedure outlined by Behar-Levy and Avnir,<sup>1</sup> we dissolved 3.398 g (20 mmol) of  $\text{AgNO}_3$  in about 50 mL of triple distilled water (TDW) in a 100 mL volumetric bottle. To this was added 0.1 mmol of Congo red (69.7 mg) dissolved in about 25 mL of TDW, and the volume was completed to 100.0 mL with pure TDW. The solution was transferred to an Erlenmeyer bottle and stirred for at least 10 min, at which point 1.320 g (15 mmol, a 50% excess of reductant) of sodium hypophosphite was added. Precipitation is immediately evident. The bottle was covered to protect it from ambient light, and the solution was stirred for 4 days (about 96 h), at the end of which the resulting powder was filtered in a glass sinter, washed with 6 portions of 25 mL, and left to dry under vacuum. The resulting product weighed 99% of the theoretical maximum (Ag + dopant). The organic loading of the CR@Ag, determined by weight loss under thermogravimetric analysis, was 2.6 wt %, which translates to a molar entrapment ratio of 240 mols of metal atoms per mol of CR. Thermogravimetric analysis (TGA) was performed with a Mettler-Toledo TGA/SDTA 851e. Experiments were run from 50 to 800 °C at 10 °C/min, under a flow of 50 mL/min dry air.

Pure silver samples were prepared identically to the above but without addition of dopant. These were also examined by TGA, and showed negligible weight loss.

**Electrochemical Analysis Setup.** Electrochemical analysis was performed using a BASi Epsilon electrochemical analyzer. The cell was a three-electrode setup with a Pt wire auxiliary electrode and an Ag/AgCl reference electrode, MF-2052 RE-5B from BASi ( $E = +0.196 \text{ V}$  vs the Standard Hydrogen Electrode according to manufacturer). All experiments were carried out in deaerated 0.01 M  $\text{KNO}_3$  as supporting electrolyte.

Working electrodes were prepared as follows: 500.0 mg of composite powder was pressed into a metallic coin 12.5 mm in diameter in an International Crystal Laboratories press, under a pressure of  $\sim 10$  tons-on-ram or 8200–8400 psi. The resulting coin was set into a holder as described in Scheme 1.

Before the first measurement on a certain day, the examined coin was polished to a mirror finish with Microcut Silicon Carbide P4000 grinding paper (Beuhler) to reveal a fresh surface (note this is not expected to achieve a particularly smooth surface; since the coins are aggregated powders, surface roughness remains relatively high). The electrode was usually not polished again (usually 2 runs were carried out in a day);

since the potentiometric procedure is not expected to significantly alter the surface, washing with TDW was sufficient. Prior to potentiometric measurements, a galvanostatic oxidation step ( $1 \text{ sec} \times 0.2 \text{ mA}$ ) was applied to remove surface contaminants. This releases a negligible amount of  $\text{Ag}^+$  into the solution ( $3.5 \times 10^{-7} \text{ M}$ ). The effect of preliminary treatments on the potentiometric response of electrodes was found to be minor (see below).

Disposable polypropylene tips with drawn-out ends were filled with supporting electrolyte solution and connected to the porous plug at the end of the commercial reference electrode, serving as Luggin capillaries to minimize potential drop due to solution resistance (relevant in voltammetry, since potentiometry involves negligible currents). The narrow end was positioned near the working electrode, though the exact distance varied; this is not important in potentiometric measurements, but in cyclic voltammetry solution resistance was electronically compensated. Chloride ion contamination is negligible: the diffusion coefficient of  $\text{Cl}^-$  is  $D = 2.032 \times 10^{-5} \text{ (cm}^2\text{)/(s)}$  (25 °C, infinite dilution<sup>15</sup>); from  $\delta = (\pi Dt)^{1/2}$ , taking the diffusion layer thickness  $\delta = 6 \text{ cm}$  (approximate capillary length), the time required for significant penetration of chloride ions into the cell is approximately 157 h, well above the experiments' duration.

$\text{N}_2$  was bubbled through TDW (to humidify the gas) and then through 6 mL of 0.01 M  $\text{KNO}_3$  for at least 10 min prior to each experiment. Thereafter the bubbling tip was raised above the solution to blanket it with inert gas. The luggin capillary solution and the added  $\text{Ag}^+$  solution (for potentiometric measurements, see below) were similarly deaerated.

**Potentiometry and Cyclic Voltammetry.** The open-circuit potential (OCP) was measured versus time; every 4 min, progressively larger volumes of deaerated  $4.63 \times 10^{-4} \text{ M AgNO}_3 + 0.01 \text{ M KNO}_3$  solution were added to the solution, which was stirred constantly at 1000 rpm to ensure efficient mass transfer and equilibration. The result is a stepped graph from which OCP values are easily extracted. Temperature did not vary by more than 2 degrees during an experiment, and "spot" measurements of solution pH before and after some of the experiments showed no significant change in pH. The electrode response was measured over a concentration range spanning almost 2 orders of magnitude, with  $\text{Ag}^+$  concentrations kept low relative to the supporting electrolyte (typically no more than  $2 \times 10^{-4} \text{ M}$  vs 0.01 M  $\text{KNO}_3$ ), to keep activity coefficients virtually constant throughout the experiment. We note that the literary activity coefficient found for pure 0.01 M  $\text{KNO}_3$  solution is 0.896,<sup>15</sup> values calculated for solution compositions throughout the experiment using Debye–Hückel models give an activity of 0.89–0.90, with negligible variation as a function of  $\text{Ag}^+$  concentration. The ionic strength is thus no more than a constant correction:  $(RT)/(F) \ln 0.9 = -2.7 \text{ mV} \Rightarrow 0.058 \text{ V} \cdot \log a_{\text{Ag}^+} = 0.058 \text{ V} \cdot \log C_{\text{Ag}^+} - 2.7 \text{ mV}$  (at  $T = 20^\circ\text{C}$ ), and it is justifiable to plot potentiometry results versus  $\log(\text{concentration})$ , as is done throughout this report. Since the distribution of results obtained is not normal, a rough estimate of the upper limit was obtained by drawing a straight line between the most positive low-concentration and high-concentration potential values. A lower limit was similarly obtained from the least positive values. Finally, the potentiometric responses of polished Ag, polished and unpolished CR@Ag electrodes after preliminary treatments of both oxidation (a galvanostatic oxidation step,  $8 \text{ sec} \times 0.2 \text{ mA}$ ) and reduction (a voltammetric sweep from the OCP to the OCP-500 mV, rate 100 mV/sec) were measured and showed that the potentiometry system is robust and its sensitivity to various preliminary treatments is minor.

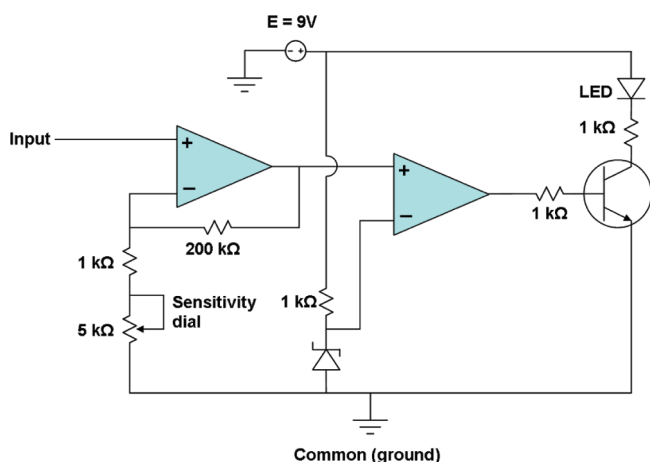
Cyclic voltammetry (CV) was performed in silver-ion free, deaerated 0.01 M  $\text{KNO}_3$ , with the sweep proceeding 500 mV from the open-circuit potential in the cathodic direction only, to avoid dissolution of the electrode. CV of CR@Ag was also performed in deaerated 0.01 M  $\text{KNO}_3 + 1.5 \times 10^{-4} \text{ M CR}$  for control purposes. The solutions were not stirred; the scan rate was 100 mV/sec.

**“Seeing the Light” Device.** The electronic circuit for the device used to create the electrochemical cell for the “seeing the light” proof of concept is described in Scheme 2. A pure Ag coin was connected to the ground in the diagram, and a CR@Ag coin or alternately, a pure Ag coin from another batch, was connected to the input. Both coins were then placed in the electrolyte, a lemon or alternately,  $3 \mu\text{M AgNO}_3 + 0.01 \text{ M KNO}_3$  solution. A dial was used to fine-tune the device sensitivity, but once set, it was of course not altered between coins. In the latter electrolyte solution of  $\text{AgNO}_3 + \text{KNO}_3$ , the difference measured by potentiostat between CR@Ag and Ag was about 55 mV at open circuit, dropping  $\sim 3 \text{ mV}$  in the course of the 60 s measurement; the difference between the two different batches of Ag was about 30 mV. The current measured between CR@Ag and Ag, when holding the potential difference constant at 0 mV, was relatively stable at  $5 \mu\text{A}$  over 60 s; the current between the two batches of Ag was  $1 \mu\text{A}$ .

## RESULTS AND DISCUSSION

**Potentiometry of Pure Ag.** The principal experimental procedure utilized in this study was measurement of the potentiometric response of the open-circuit potential (OCP) of the working electrodes, pure and doped silver, to a solution of silver ions at varying concentrations. The plot of the OCP versus the logarithm of the ion activity in solution is expected to be linear, in

**Scheme 2. Electronic Circuit Design for the “Seeing the Light” Device**



accordance with Nernst’s law. The intercept of this line indicates the electrode potential, and the slope depends on the characteristics of the reaction at the interphase between the electrode and the electrolyte. Potentiometric measurements have the advantage of simplicity, involving no electrolytic change of the working electrode surface. In addition, the potential drop due to solution resistance is negligible ( $i = 0 \Rightarrow V_{sol} = iR_{sol} = 0$ ), allowing for greater reproducibility. This is seen in Figure 1a, where repeated measurements of two different yet identically prepared batches of pure silver demonstrate that the system is generally well behaved. Figure 1b shows average values calculated from these measurements, with an estimation of uncertainty.

Linear behavior is indeed kept over most of the range, deviating from linearity only near the detection threshold. Fitting of the average data (Figure 1b) in the higher decade ( $10^{-4.8} \text{ M} - 10^{-3.8} \text{ M}$ ), where linearity is better kept, yields a slope of 49 mV, as opposed to the Nernstian 58 mV for a single-electron, one-step reaction at  $20^\circ\text{C}$ . This sub-Nernstian response resembles the behavior of silver-ion selective electrodes (see for example Chung et al.,<sup>16</sup> Lim et al.,<sup>17</sup> Badr<sup>18</sup>), commonly attributed in such studies to the particulars of the ion-selective properties of the electrode. In the present case the highly porous, aggregated nature of the electrode may give rise to an analogous diffusion-related potential drop. An experiment performed in the same system with a polycrystalline pure Ag wire electrode (not shown) yielded a slope of 55 mV/decade, much closer to the expected Nernstian slope, lending credence to this idea. The detection threshold of the system is about  $10^{-5.5} \text{ M}$ , which is similar to the threshold of the Ag wire system just mentioned and comparable to the detection limits of silver in ion-selective potentiometry literature, which are typically not lower than  $10^{-6} - 10^{-7} \text{ M}$ .<sup>16–20</sup> The intercept extracted from the higher-concentration decade linear fit (corrected for activity) is +0.52 V versus the reference Ag/AgCl electrode, or +0.72 V versus the Standard Hydrogen Electrode. The deviation of this value from the literary +0.796 V for silver is reasonable, considering that the extrapolation of these results to unit activity is highly sensitive to small variations in the slope, making the intercept values attained in this methodology generally unreliable.

**Potentiometry of CR@Ag.** The results of potentiometric characterization of the CR@Ag electrode, that is silver doped with the dye Congo red (CR), are shown in Figure 2a. The comparison of the average values with those of pure Ag are shown in Figure 2b.

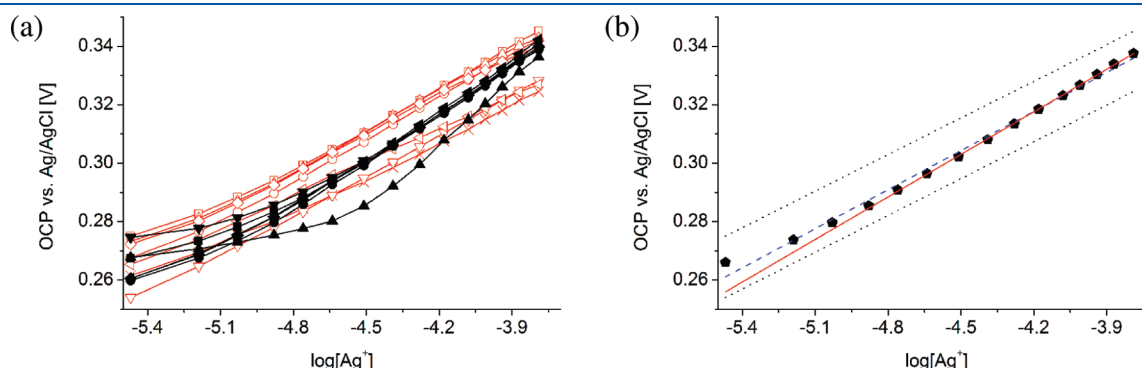


**Figure 1.** Open-circuit potential (OCP) of pure Ag in equilibrium with  $\text{Ag}^+$  solution. (a) Individual results of measurements on two different batches (hollow and filled dots, the lines are for illustration purposes only) of identically prepared Ag. (b) Average values (dots); estimated uncertainty, based on the limiting results (dotted lines); linear curves fitted to all the data (dashed line,  $R^2 = 0.9969$ , slope = 45 mV/decade, intercept = 505 mV) and to the high-concentration decade (solid line,  $R^2 = 0.9997$ , slope = 49 mV/decade, intercept = 521 mV).

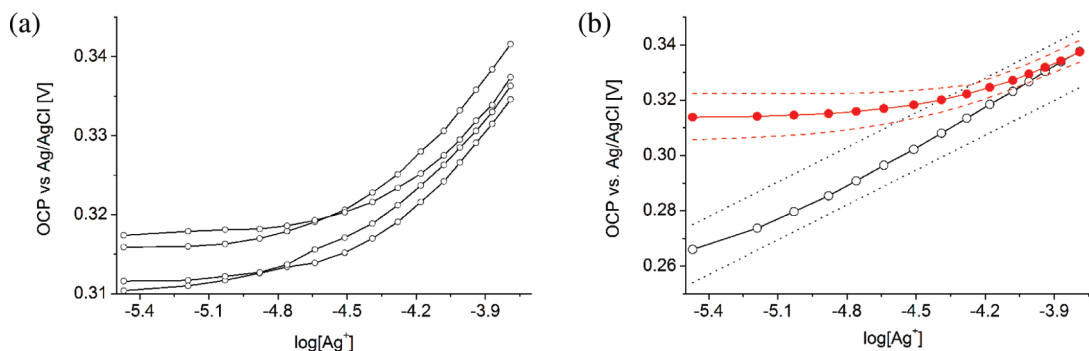


**Figure 2.** Open-circuit potential (OCP) of CR@Ag in equilibrium with  $\text{Ag}^+$  solution. (a) Results of individual measurements (the lines are for illustration purposes only). (b) Average values of OCP measurements for CR@Ag (filled dots); estimated uncertainty, based on limiting results (dashed lines). Also shown are average OCP values for pure Ag (hollow dots) and estimated uncertainty in pure Ag measurements, based on the limiting results (dotted lines).

Figure 2b points out a significant, reproducible alteration of electrode behavior, namely, the loss of electrode response to changes in  $\text{Ag}^+$  concentration at low ion concentrations. In other words, the incorporation of CR into the electrode causes a significant increase of the detection threshold for silver ion: the weak response of pure Ag electrodes to changes in  $\text{Ag}^+$  concentration at the lowest  $\text{Ag}^+$  concentrations examined (around  $10^{-5.5}$  M) is only recovered at concentrations more than 1.5 decades (30 times) higher in the CR@Ag electrode.

Several factors may affect the detection threshold of an electrode. The weak response below the threshold of silver ion-selective electrodes based on a thick film of silver sulfide has been attributed to the weakly defined presence of impurities in background electrolyte and to the adsorption of silver ions on the walls of containers, which may become significant at low  $\text{Ag}^+$  concentrations.<sup>19,20</sup> Of these, adsorption to container walls in the time scale of the experiment must in our case be rejected, since it cannot be affected by the entrapment of the dopant in the CR@Ag electrode. Tani et al found in their research of  $\text{CuS}/\text{Ag}_2\text{S}$  membranes that the presence of oxygen had a detrimental effect on the sensitivity of the membranes to  $\text{Cu}^{2+}$  ions, especially in solutions containing triethylenetetramine (trien).<sup>21</sup> They concluded that the loss of sensitivity and higher membrane potentials observed were caused by a process of membrane oxidation by the dissolved oxygen. A similar idea was suggested by Meruva and Meyerhoff as the main potentiometric response mechanism of copper thin films to  $\text{O}_2$ .<sup>22</sup> They suggested that the potentials measured at such films arise from a *mixed* (or corrosion) potential which results from the steady-state oxidation of the copper film and simultaneous reduction of the dissolved oxygen.

In our case, the idea of a mixed-potential system (as opposed to an equilibrium system) is plausible, and as will be seen below, it is supported by the results of our voltammetric measurements. While it is difficult without more information to speculate on the nature of the competing reaction involved, a likely candidate is the reduction of residual oxygen (which remains despite prior deaeration with  $\text{N}_2$ ).

**Voltammetry of CR@Ag.** Our observation from potentiometry experiments has been that at low  $\text{Ag}^+$  concentrations the measured potential does not match the  $\text{Ag}^+/\text{Ag}$  equilibrium potential and does not depend on silver ion activity, and that as silver concentrations rise, a gradual transition to Nernstian behavior occurs. Such gradual transition is well described in terms of mixed potential, as follows: Given that silver reduction

and oxidation are simultaneously occurring, let us assume in addition an interfering cathodic reaction (such as oxygen reduction) which is more facile than the silver ion reduction at low  $\text{Ag}^+$  activity. Analysis (see appendix) then yields the following behavior:

$$E = E^{0'} + \frac{0.058V}{\alpha_a + \alpha_{c,i}} \log a_{ox,i}$$

Here,  $E$  is the measured potential,  $\alpha_a$  and  $\alpha_{c,i}$  are the transfer coefficients for the anodic silver dissolution and the cathodic interfering reaction, respectively, and  $\alpha_{ox,i}$  is the activity of the interfering species undergoing reduction.  $E^{0'}$  is thus the *mixed* potential, at unit activities, of the system. It arises from a steady state of silver oxidation and the interfering reduction, lying in between the reversible potentials of the reactions involved. Note that the  $\text{Ag}^+$  concentration at which the transition to normal Nernstian behavior occurs depends on the rate of the interfering reaction. In light of this, the interesting observation follows, that the competing reaction has been catalyzed by the composite. A similar behavior appears, for example, in the case of  $\text{CuS}/\text{Ag}_2\text{S}$  membranes in  $\text{Cu}^{2+}$  solutions: in those systems, the deterioration of the detection threshold was attributed to acceleration of membrane corrosion by oxygen in solutions containing trien.<sup>21</sup> In similar fashion, we propose that CR entrapment has accelerated the reduction of oxygen on the surface of the electrode; oxygen activation was observed in thermally activated CR@Ag for methanol oxidation to formaldehyde.<sup>13</sup> It follows from the mixed-potential model that at a given applied negative potential, and in the absence of  $\text{Ag}^+$ , a reduction current should be observed (“negative applied potential” in this section is defined relative to the open-circuit potential). Furthermore, the current measured at the CR@Ag electrode should be greater, by the factor by which the reaction’s rate constant was increased.

CR@Ag and Ag in 0.01 M  $\text{KNO}_3$  were subjected to cyclic voltammetry (CV) analysis. The sweep proceeded from the open-circuit potential in the cathodic direction only, to avoid dissolution of the electrode. The resulting voltammogram is presented in Figure 3. Also shown is the current measured at the pure Ag electrode, scanned in dilute ( $1.5 \times 10^{-4}$  M) CR solution.

It is immediately apparent that the behavior of CR@Ag is significantly different from that of pure Ag. Figure 3b shows an enlarged view of the two curves for pure Ag, with or without the presence of dilute CR; though there is considerable noise in the

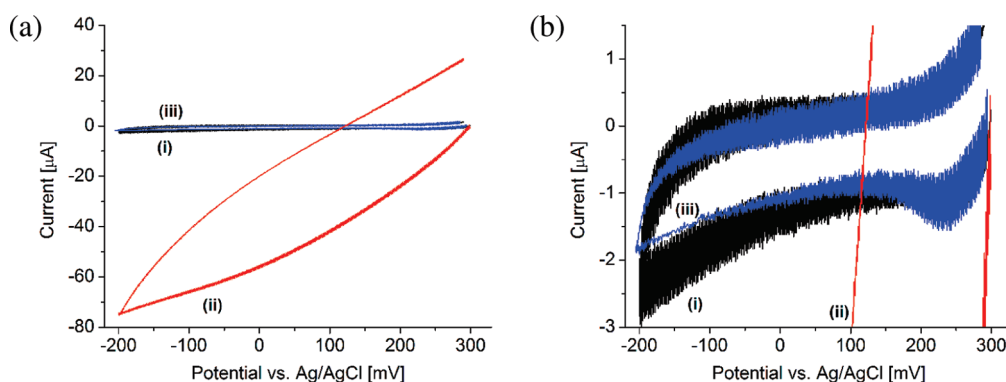


**Figure 3.** (a) Cyclic voltammetry of electrodes in 0.01 M  $\text{KNO}_3$ : (i) pure Ag; (ii) CR@Ag; (iii) pure Ag in  $\text{KNO}_3 + \text{CR}$  ( $1.5 \times 10^{-4}$  M). (b) Same as (a), low-current range enlarged; note that (i) and (iii) overlap greatly. Scan rate: 100 mV/sec, solution not stirred.

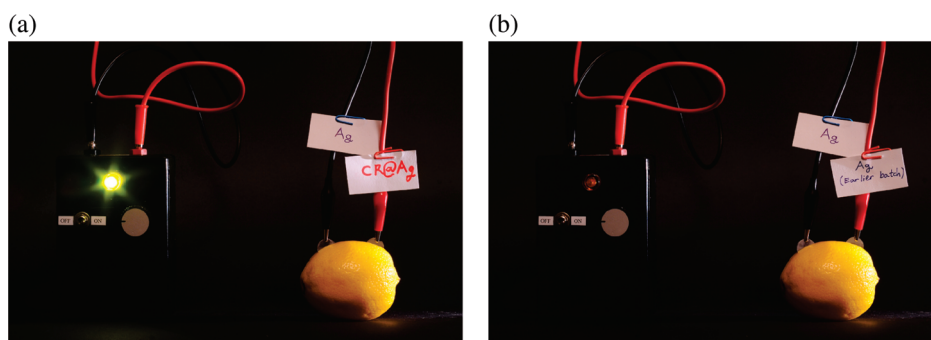


**Figure 4.** “Seeing the light” proof of concept. (a) CR@Ag vs pure Ag; (b) pure Ag from an earlier batch vs the pure Ag from (a).

measurement, it is evident that the two curves closely resemble each other, in stark contrast to the curve for CR@Ag. This implies that the altered behavior is a unique result of the incorporation of CR into the electrode. It also shows that free CR in solution does not undergo reduction in the potential range scanned. This last is expected; electrochemical studies in literature of CR and Acid Orange 7, a similar azo dye, indicate that reduction of the dye, at similar or even higher concentrations than that used here, does not occur before  $-0.5$  V versus Ag/AgCl.<sup>23,24</sup>

The curve for CR@Ag (curve (ii)) shows a large hysteresis between the forward and the reverse scans. The most likely explanation for this is the roughness of the electrode surface, leading to a large capacitive (nonfaradaic) current. Organics@metals materials are indeed known to be porous;<sup>1</sup> it appears that the pressure applied when pressing the CR@Ag powder into coins is not sufficient to seal off many of the pores, leading to a high actual surface area.

However, since purely capacitive anodic and cathodic currents are expected to be symmetrical around the null-current axis, it is evident that beyond the charging current, some *net reduction* current flows at negative potentials. This is what we would expect if some species from solution was undergoing reduction; this species can obviously not be silver, since the solution was devoid of  $\text{Ag}^+$ . On an ideally flat electrode surface, the CV trace might uncover clear features of the reduction curve that could be useful in determining the identity and bulk concentration of the species being reduced; however, the high electrode roughness results in a situation where diffusional mass-transport to the surface occurs in an ill-defined manner, which is determined by the (possibly depth-dependent) effective diffusion coefficient inside the CR@Ag matrix.

Thus, the classic peak shape appearing in CV curves on well controlled, flat surfaces is replaced with a steady, almost linear rise in current with more negative potential. This is, incidentally, much less pronounced on the pure Ag electrode surface (see the enlargement, Figure 3b), where the capacitive current is also much lower and so, presumably, the roughness. However, here the fine details of the reduction process are hard to discern because of the small signal-to noise ratio.

A comparison, once the capacitive current is accounted for, of the curves for CR@Ag and pure Ag (with or without the presence of CR in solution) shows that the currents obtained throughout the CV sweep of CR@Ag are roughly 30 times larger than those obtained from pure Ag. This matches nicely the 1.5-decade higher  $\text{Ag}^+$  concentration required to recover a Nernstian response from CR@Ag (Figure 2b), lending credence to our working hypothesis.<sup>25</sup>

“Seeing the Light”. The foregoing results form the fundament for a new kind of electrochemical cell, based on the concept of metal doping. The alteration of electrode behavior by doping means that pure and doped (or two differently doped) metal electrodes may be placed in an electrolyte and connected by an external circuit, and the (doping-based) potential difference arising may be used to drive a current through it, gate an electronic component, and so forth. The proof of this concept was carried out, and is presented in Figure 4: in the setup shown, coins of pure Ag and CR@Ag (or pure Ag from an earlier batch) serve as the electrodes, and are placed in an electrolyte—a lemon. The external circuit chosen includes a light-emitting diode (LED) which is driven by an external source; the potential difference between the electrodes is amplified and used to gate this component (see details in the Experimental Section and Scheme 2). When CR@Ag and

pure Ag coins are connected to the circuit, the potential difference between them suffices to trigger the lighting of the LED (subfigure (a)); when coins from two different batches of pure Ag are connected to the circuit, the LED does not light (subfigure (b)). This experiment was also performed with a more conventional electrolyte of  $\text{AgNO}_3 + \text{KNO}_3$  (3  $\mu\text{M}$  and 0.01 M respectively, similar to the electrolyte composition at the low-concentration end of the potentiometry measurements), yielding similar results. The potential difference in the latter case was measured by the potentiostat at about 55 mV (the potential difference in the lemon was not measured; see more details in the Experimental Section).

## CONCLUSION

The results shown in this report culminate in the “seeing the light” proof of concept, which demonstrates the alteration of the electrode behavior of a metal by entrapment of a dopant. The apparent reduction potential of the electrode is affected by doping in an indirect way, that has its root in catalysis of a competing reaction in the solution, which may be speculated to be the reduction of residual oxygen. The “seeing the light” experiment introduces the concept of a doping-based electrochemical cell. In contrast to a Galvanic cell, which is based on a free energy difference between the reactions occurring at the two electrodes in the cell, the electrochemical cell constructed here is based rather on a kinetic difference. Under the assumptions of this analysis, the same corrosion process occurs at both electrodes, involving the same metal in both electrodes, which are also placed in the same electrolyte; however, by virtue of metal doping, the process occurs more quickly at one of the electrodes, and this creates a potential difference. If a motivational example is desired, consider that the common approach to electrochemical cells would attempt to separate the reduction and oxidation reactions occurring at a single electrode into separate half-cells and take advantage of the spontaneously occurring corrosion reaction. However, such separation might not be trivial; for example, the corrosion reaction may occur exclusively on a silver surface. Thus, the metal–organics@metal cell concept may well open up new vistas for battery and fuel-cell research.

## APPENDIX: KINETIC ANALYSIS OF A MIXED-POTENTIAL SYSTEM

Consider a system where a reaction of interest and another, interfering reaction both occur. The measured current density  $i$  is the sum of the anodic and cathodic currents,

$$\begin{aligned} i &= i_a - i_c + i_{a,i} - i_{c,i} \\ &= Fa_{red}k_a \cdot \exp\left[\frac{F}{RT}\alpha_a\Delta\varphi\right] - Fa_{ox}k_c \cdot \exp\left[-\frac{F}{RT}\alpha_c\Delta\varphi\right] \\ &\quad + Fa_{red,i}k_{a,i} \cdot \exp\left[\frac{F}{RT}\alpha_{a,i}\Delta\varphi\right] - Fa_{ox,i}k_{c,i} \cdot \exp\left[-\frac{F}{RT}\alpha_{c,i}\Delta\varphi\right] \end{aligned}$$

Here,  $i_a$  and  $i_c$  are the currents arising from the anodic and cathodic reaction, respectively,  $\Delta\varphi$  is the potential drop on the electrode–electrolyte interphase,  $k_a$  and  $k_c$  are the chemical rate constants at  $\Delta\varphi = 0$ , and  $a_{red}$  and  $a_{ox}$  are the activities of the reduced and oxidized species, respectively.  $\alpha_a$  and  $\alpha_c$  are the anodic and cathodic transfer coefficients, which should be treated as experimental parameters and are used in preference to the reactions’ symmetry factors, as these are not measurable in multistep electrode processes.<sup>26</sup> Notations for the interfering reaction include  $i$  subscripts.

In potentiometric measurements, the measured current is 0. Setting  $a_{red} = 1$  (the activity of solid silver),  $a_{ox} \equiv a_{\text{Ag}^+}$ ,

$$\begin{aligned} 0 &= Fk_a \cdot \exp\left[\frac{F}{RT}\alpha_a\Delta\varphi\right] - Fa_{\text{Ag}^+}k_c \cdot \exp\left[-\frac{F}{RT}\alpha_c\Delta\varphi\right] \\ &\quad + Fa_{red,i}k_{a,i} \cdot \exp\left[\frac{F}{RT}\alpha_{a,i}\Delta\varphi\right] - Fa_{ox,i}k_{c,i} \cdot \exp\left[-\frac{F}{RT}\alpha_{c,i}\Delta\varphi\right] \end{aligned}$$

To advance, the assumption is made that the interfering cathodic reaction proceeds rapidly in relation to both the interfering anodic reaction and the reduction of silver; the latter condition applies at sufficiently low concentrations of  $\text{Ag}^+$ . In other words,  $a_{red,i}k_{a,i} \ll a_{\text{Ag}^+}k_c \ll a_{ox,i}k_{c,i}$ , and thus the two middle terms vanish and the expression becomes:

$$\begin{aligned} 0 &= Fk_a \cdot \exp\left[\frac{F}{RT}\alpha_a\Delta\varphi\right] - Fa_{ox,i}k_{c,i} \cdot \exp\left[-\frac{F}{RT}\alpha_{c,i}\Delta\varphi\right] \\ \Rightarrow \ln k_a + \frac{F}{RT}\alpha_a\Delta\varphi &= \ln a_{ox,i} + \ln k_{c,i} - \frac{F}{RT}\alpha_{c,i}\Delta\varphi \\ \Rightarrow (\alpha_a + \alpha_{c,i})\Delta\varphi &= \frac{RT}{F} \ln \frac{k_{c,i}}{k_a} + \frac{RT}{F} \ln a_{ox,i} \end{aligned}$$

Setting for a moment  $a_{ox,i} = 1$ , this becomes  $RT/F \ln(k_{c,i}/k_a) \equiv (\alpha_a + \alpha_{c,i})\Delta\varphi^{0'}$ , and thus  $\Delta\varphi^{0'}$  indicates the potential difference across the metal-solution interphase at unit activity of all components. The interphase potential difference,  $\Delta\varphi$ , is not directly measurable, but changes in this potential are measurable, that is,  $\Delta\varphi - \Delta\varphi^{0'} = E - E^{0'}$ . Therefore, one may write:

$$\begin{aligned} \Delta\varphi &= \Delta\varphi^{0'} + \frac{1}{\alpha_a + \alpha_{c,i}} \cdot \frac{RT}{F} \ln a_{ox,i} \\ \Rightarrow E &= E^{0'} + \frac{1}{\alpha_a + \alpha_{c,i}} \cdot \frac{RT}{F} \ln a_{ox,i} \\ \Rightarrow E &= E^{0'} + \frac{0.058V}{\alpha_a + \alpha_{c,i}} \cdot \log a_{ox,i} \end{aligned}$$

$E^{0'}$  is the mixed potential, at unit activities, of the system. The measured potential,  $E$ , is not an equilibrium potential, but rather the potential arising from a steady state of simultaneous silver oxidation and an interfering reduction, so that no current flows in the external circuit.

## AUTHOR INFORMATION

### Corresponding Author

\*E-mail: david@chem.ch.huji.ac.il.

## ACKNOWLEDGMENT

The authors thank Prof. Ovadia Lev of the Hebrew University for many helpful discussions, without which this work would never have been completed. We thank the electronics lab of the Institute of Chemistry for valuable help in the construction of the “seeing the light” device. Finally, we thank a reviewer for a valid and useful suggestion. This work was supported by the Tashtiot Program of the Israel Ministry of Science.

## REFERENCES

- (1) Behar-Levy, H.; Avnir, D. *Chem. Mater.* **2002**, *14*, 1736–1741.
- (2) Neouze, M.-A.; Litschauer, M. *J. Phys. Chem. B* **2008**, *112*, 16721–16725.
- (3) Ben-Knaz, R.; Avnir, D. *Biomaterials* **2009**, *30*, 1263–1267.

- (4) Duran Pachon, L.; Yosef, I.; Markus, T. Z.; Naaman, R.; Avnir, D.; Rothenberg, G. *Nat. Chem.* **2009**, *1*, 160–164.
- (5) Nesher, G.; Aylien, M.; Sandaki, G.; Avnir, D.; Marom, G. *Adv. Funct. Mater.* **2009**, *19*, 1293–1298.
- (6) Sinai, O.; Avnir, D. *J. Phys. Chem. B* **2009**, *113*, 13901–13909.
- (7) Ben-Knaz, R.; Pedahzur, R.; Avnir, D. *Adv. Funct. Mater.* **2010**, *20*, 2324–2329.
- (8) Yosef, I.; Avnir, D. *Chem. Mater.* **2006**, *18*, 5890–5896.
- (9) Behar-Levy, H.; Avnir, D. *Adv. Funct. Mater.* **2005**, *15*, 1141–1146.
- (10) Yosef, I.; Abu-Reziq, R.; Avnir, D. *J. Am. Chem. Soc.* **2008**, *130*, 11880–11882.
- (11) Nesher, G.; Marom, G.; Avnir, D. *Chem. Mater.* **2008**, *20*, 4425–4432.
- (12) Behar-Levy, H.; Neumann, O.; Naaman, R.; Avnir, D. Chirality induction in bulk gold and silver. *Adv. Mater.* **2007**, *19*, 1207.
- (13) Shter, G. E.; Behar-Levy, H.; Gelman, V.; Grader, G. S.; Avnir, D. *Adv. Funct. Mater.* **2007**, *17*, 913–918.
- (14) Koch, G.; Brongers, M.; Thompson, N.; Virmani, Y.; Payer, J. *Corrosion Costs and Preventive Strategies in the United States*; Report No. FHWA-RD-01-156; Federal Highway Administration: Washington, DC, 2002.
- (15) *CRC Handbook of Chemistry and Physics*, 87th ed.; Lide, D. R., Ed.; Taylor and Francis, Boca Raton, FL, 2007.
- (16) Chung, S.; Kim, W.; Park, S. B.; Kim, D. Y.; Lee, S. S. *Talanta* **1997**, *44*, 1291–1298.
- (17) Lim, S. M.; Chung, H. J.; Paeng, K.-J.; Lee, C.-H.; Choi, H. N.; Lee, W.-Y. *Anal. Chim. Acta* **2002**, *453*, 81–88.
- (18) Badr, I. H. A. *Microchim. Acta* **2005**, *149*, 87–94.
- (19) Tymecki, L.; Zwierkowska, E.; Glab, S.; Koncki, R. *Sens. Actuators, B* **2003**, *96*, 482–488.
- (20) Durst, R. A.; Duhart, B. T. *Anal. Chem.* **1970**, *42*, 1002–1004.
- (21) Tani, Y.; Soma, M.; Graf Harsanyi, E.; Umezawa, Y. *Anal. Chim. Acta* **1999**, *395*, 53–63.
- (22) Meruva, R. K.; Meyerhoff, M. E. *Electroanalysis* **1995**, *7*, 1020–1026.
- (23) Bonancea, C. E.; do Nascimento, G. M.; de Souza, M. L.; Temperini, M. L. A.; Corio, P. *Appl. Catal., B* **2006**, *69*, 34–42.
- (24) Stanoeva, T.; Neshchadin, D.; Gescheidt, G.; Ludvik, J.; Lajoie, B.; Batchelor, S. N. *J. Phys. Chem. A* **2005**, *109*, 11103–11109.
- (25) It has been suggested by a reviewer that the large capacitive current may offer an alternative explanation, namely, that the resistance through the CR@Ag electrode is significantly larger than that of Ag, which would lead to an RC-circuit like behaviour, involving no reduction in solution; this is indeed a valid proposition. However, an order-of-magnitude calculation of the required resistivity leads to values in the range of semiconductor resistivities ( $\sim 10$  Ohm·meter) for CR@Ag. This is very high, considering the results of Nesher et al.'s conductivity measurements of polyaniline@Ag, in which much higher dopant loads (up to 8.5% wt as opposed to 2.6% in our CR@Ag) caused, at most, a 2-order-of-magnitude increase in the resistivity of Ag.<sup>5</sup> Note also that even if the resistance through the electrode is indeed much increased, via alteration of Ag's resistivity by doping, or by some fault of electrode construction, it must be increased such that the entire net current observed is more-or-less exactly accounted for, to invalidate our working hypothesis.
- (26) Gileadi, E. *Electrode Kinetics*; VCH: New York, 1993.